FUDMA Journal of Sciences (FJS)
ISSN online: 2616-1370
ISSN print: 2645 - 2944
Vol. 10 No. 17, September, 2026, pp 200 – 212
DOI: https://doi.org/10.33003/fjs-2026-1017-6025

Green Synthesis of Zinc Oxide Nanoparticles Using Baobab (*Adansonia digitata*) Leaf Extract for Co(II), Pb(II), and Ni(II) Removal from Synthetic and Industrial Wastewater.

***Faridah Dauda Salehkyari, *Shaibu Yusuf and Hussaini Garba**

Department of Chemistry, Sule Lamido University Kafin Hausa, Jigawa State, Nigeria.

*Corresponding authors' email: faridahkyari40@gmail.com
ORCID: https://orcid.org/0009-0000-7925-5038

ABSTRACT

This study aimed at synthesizing and characterizing Leaf ZnO nanoparticles from baobab (*Adansonia digitata*) for adsorption of Co(II), Pb(II) and Ni(II) from wastewater. Green synthesis method was carried out using a mixture 50 ml of 0.02 M zinc acetate dihydrate solution and 50 ml of plant extract under continuous stirring at constant temperature of 70 ^{0}C. The ZnO NPs were characterized using XRD, FTIR and SEM-EDX. XRD analysis confirmed the crystallinity of the synthesized ZnO nanoparticles, with crystallite sizes ranging from 12.7nm to 22.4nm. It also shows that Zn-O was the predominant crystalline phase, accounting for 90.3 wt.% ZnO. FTIR analysis showed the presence of a strong band at 551cm^{-1}, while SEM reveals the morphology of the synthesized Nanoparticles. In addition, the EDX analysis revealed Zn-O were the predominant elements present, with zinc accounting for 81.95 wt.%, and oxygen accounted for 17.54 wt.%. The results for treatments of synthetic wastewater was obtained, maximum removal efficiencies of 77.40%, 82.7% and 72.1% were achieved for Co(II), Pb(II) and Ni(II) ions respectively, under optimized conditions of pH 6, 80 min and 200 mg adsorbent dosage. Increasing the initial metal concentration decreased removal efficiency while interfering ions enhanced Co^{2+} removal but reduced Pb^{2+} and Ni^{2+} adsorption. The results for the treatment of industrial wastewater for Co^{2+}, Pb^{2+} and Ni^{2+} ions adsorption using the synthesized NPs gave a maximum adsorption efficiencies of 80.10%, 68.33%, and 63.92%, respectively) at the same experimental conditions. The results showed that synthesized ZnO-nanoparticles effectively removed these heavy metals from solution.

Received: 14 Sept. 2026
Accepted: 17 Sept. 2026
Published: 23 Sept. 2026

Keywords: Baobab(*Adansonia digitata*), Zinc Oxide Nanoparticles, Cobalt, Lead, Nickel, Wastewater

INTRODUCTION

Nanotechnology has been compartmentalised into areas like chemical, pharmaceutical, mechanical and food processing industries. It also contributes in areas such as power generation, optics, drug delivery, and environmental sciences (Shah *et al.,* 2021). Since the start of nanotechnology, a lot of nanoscale devices have been produced using different techniques like physical, chemical, and green approaches. Even though, green nanoparticle synthesis is a tool of choice that can be easily developed and monitored (Muhammad *et al.,* 2021), there are many challenges associated with the conventional methods use for the synthesis of nanoparticles. Some these include high cost, tedious procedures, and most importantly the use of harmful compounds. In the recent past efforts have been directed toward eco-friendly and rapid synthesis processes for the development of nanoparticles as a result of these limitations (Kumar *et al.,* 2015). In this regards, green synthesis of nanoparticles using plant extracts is the centre of focus, because it simple, cheap, and use nontoxic compounds (Nandi and Hassan 2015). Moreover, green synthesis methods have more advantages over other classical synthesis methods due to the availability biological substrates and eco-friendly procedures. The rich biodiversity and availability of plant materials have been highly explored for the nanoparticles synthesis (Monda *et al.,* 2011).

Extracts from various plant components, including geranium leaves, lemon grass, neem leaves and Aloe vera have been utilized for this purpose (Rajkumari *et al.,* 2017).

In the textile industry, various organic colour dyes have been extensively used, resulting in the generation of a considerable amount of wastewater containing toxic and vibrant dyestuffs during manufacturing. This has led to the pollution of surface and groundwater. Various physical and chemical processes have been employed to address this issue to remove these hazardous contaminants. These processes include electrocoagulation (Jha *et al.,* 2009), flocculation /coagulation (Huang *et al.,* 2007).

Heavy metal contamination of water is a serious environmental problem due to the persistence and potential toxicity of metals such as Pb(II), Ni(II) and Co(II). Their presence in wastewater can pose risks to human health and aquatic ecosystems, making their effective removal essential. Existing methods for heavy-metal removal may be costly, require toxic chemical inputs, or generate secondary waste. Although adsorption is considered a simple and effective treatment method, the performance of an adsorbent depends strongly on its surface properties and operating conditions.

In the preparation of dyes, certain amount of heavy metals like copper, chromium, cobalt, or nickel are added. The presence of these heavy metals in the dye molecule enables the dye to be applied more easily to the fibre, leading in a faster dyeing process. However, when wastewater from a dying industry is not treated before disposal it contaminates the environment. Moreover, untreated dye wastewater has been reported to contaminate river Noyyal and Buriganga in Tiruppur (India) and Dhaka (Bangladesh) making them unsuitable for irrigation as result of heavy metal accumulation Abirami *et al.,* (2024).

ZnO nanoparticles have potential for heavy-metal adsorption because of their active surface sites and high surface area. However, conventional methods of producing nanoparticles may involve hazardous chemicals and energy-intensive processes. There is therefore a need for safer and more environmentally friendly methods of ZnO nanoparticle synthesis.

Adansonia digitata (baobab) is a locally available plant with diverse phytochemicals that can support the green synthesis of nanoparticles. Previous studies have demonstrated the synthesis and characterization of ZnO nanoparticles using *Adansonia digitata* leaf extracts, while other studies have investigated their application for the removal of selected heavy metals. However, limited information is available on the application of baobab-leaf-derived ZnO nanoparticles for the removal of Co(II), Pb(II) and Ni(II) particularly from wastewater associated with textile and local cloth-dyeing activities. Therefore, this study aimed to synthesize and characterise ZnO nanoparticles from baobab (*Adansonia digitata*) Leaf extracts and evaluate their effectiveness for the adsorption of Co(II), Pb(II) and Ni(II) from synthetic and industrial wastewater.

MATERIALS AND METHODS

Samples Collection

Fresh baobab (*Adansonia digitata*) leaf was collected from a healthy tree within Kafin Hausa area of Jigawa State Nigeria. Industrial wastewater was collected from local cloth dyeing sites in Hadeja Local government of Jigawa State in clean polyethylene containers. The samples were transported to the laboratory and stored under appropriate conditions prior to analysis and adsorption experiments.

The materials and chemicals used in this study was Baobab (*Adansonia digitata)* leaf, Zinc acetate dihydrate ($Zn(CH_3COO)_2.2H_2O$, Sodium hydroxide, Distilled-deionized water, lead acetate trihydrate $Pb(CH_3COO)_2.3H_2O$, nickel chloride hexahydrate $NiCl_2.6H_2O$ and cobalt (II) nitrate hexahydrate $Co(NO_3)_2.6H_2O$, Sodium chloride, calcium chloride, Ferric chloride, Whatman filter paper, pH meter, Magnetic stirrer, Centrifuge, Drying oven, Muffle furnace, Atomic absorption spectrophotometer, Standard laboratory glass wares and thermometer

Preparation of Plants Materials

The collected leaf was washed thoroughly with tap water followed by distilled water to remove dust and impurities and further rinsed with deionized water. The samples were air dried for 7 days, ground into fine powder using laboratory grinder and stored in airtight containers**.**

Preparation of Plants Extract

Exactly 10g of powdered leaf was mixed with 100 ml of distilled water and heated at a constant temperature of 70˚C with continuous stirring for 1 hour, the mixture was allowed to cool and was filtered using Whatman No. 1 filter paper. A clear filtrate which served as reducing and stabilizing agent during nanoparticles synthesis was obtained for ZnO nanoparticle synthesis, following modified procedure reported by (Siddiqi *et al.,* 2018).

Green Synthesis of Zinc Oxide Nanoparticles

Exactly 50 ml of 0.02 M zinc acetate dihydrate ($Zn(CH_3COO)_2.2H_2O$, solution was measured and mixed with 50 ml of the plant extract under continuous magnetic stirring at 70 ^{0}C for 2 hours. Then 0.2 M of Sodium hydroxide (NaOH) solution was added drop wise until a white milky precipitate was observed at pH 10. The solution was allowed to stand for 24 hours, decanted and centrifuged at 8,000 rpm for 15 minutes. The precipitates were washed repeatedly with distilled water, oven dried and calcine at 550˚C for 3 hours, ZnO nanoparticles was obtained (Majeed *et al.,* 2019; Masoud *et al.,* 2022).

Preparation of Synthetic Wastewater

Stock standard solution of synthetic wastewater containing 20 mg/L each of lead, nickel and Cobalt ions was prepared from $Pb(CH_3COO)_2.3H_2O$, $NiCl_2.6H_2O$ and $Co(NO_3)_2.6H_2O$ respectively using distilled-deionized water. Moreover, 10 mg/L, 20 mg/L, 30 mg/L, 40 mg/L and 50 mg/L of the different salts solutions were prepared and used in the adsorption experiments.

Determination of Initial Heavy Metal Concentration

Prior to adsorption both the synthetic and the collected industrial wastewater samples were analysed using AAS to determine the initial and final concentration of the metals following standard analytical procedures for water quality assessment (APHA, 2017).

Batch Adsorption Experiment

Batch adsorption studies were performed with various parameters: initial pH value (2.0, 4.0 and 6.0), adsorbent dosage (50, 100, 200 and 30mg, Co(II), Pb(II) and NI(II) concentrations (10, 20, 30, 40 and 50 mg/L) and contact time (20, 40, 60 and 80 min). The experiments were conducted in 50 ml Erlenmeyer flasks with 20 ml working Co(II), Pb(II) and NI(II) solution each. The adsorption process was conducted on a rotary shaker with a magnetic stirrer at ambient (32 ^{0}C) temperature. After reaching the desired contact time, the mixture was centrifuged for 15 min at 8000 rpm, the supernatant was filtered through a 0.45 μm filter membrane, and the Co(II), Pb(II) and NI(II) concentrations were determined using flame atomic absorption spectroscopy (Perkin Elmer AA800, USA). Influences of each factor were examined, while others were kept constant: pH = 6.0, adsorbent dosage of 200 mg, Co(II), Pb(II) and NI(II) concentration of 50 mg/L, and contact time of 80 min were obtained as the optimal experimental conditions for this study. The removal efficiency (%removal) and adsorption capacity (qe) were calculated using the following equations, respectively (Sharma and Shukla, 2021).

Effect of Solution pH

The effect of pH on adsorption efficiency was investigated by varying the pH (2, 4 and 6) of the metal solutions while maintaining constant adsorbent dosage of 200 mg, contact time of 80 minutes and initial metal concentration of 20 mg/L. The pH range selected for the study included acidic and near neutral conditions consistent with previous adsorption optimization studies on ZnO based adsorbents (Bagheri *et al.,* 2014).

Effect of Contact Time

The effect of contact time on heavy metals adsorption was investigated through different time intervals of 20, 40 60 and 80 minutes and keeping other parameters constant. The optimum contact time obtained for each adsorbent was 80 minutes and subsequently applied later in the adsorption studies to ensure equilibrium conditions were obtained (Lagergren, 1898).

Effect of Adsorbent Dosage
The influence of adsorbent dosage was analysed by varying the amount of ZnO nanoparticles (50mg, 100 mg, 200 mg, and 300 mg) while maintaining constant pH (6), contact time (80 minutes) and initial metal concentration of (20 mg/L). This is consistent with adsorption studies showing that increased adsorbent dosage enhances available active sites for metal ion binding (Kumar *et al.,* 2017).

Effect of Initial Metal Concentration
The effect of initial metal ion concentration on adsorption was studied using different concentrations of lead, nickel and cobalt solutions each starting with 10, 20, 30 40 and 50 mg/L, while maintaining optimized adsorption conditions. Similar approaches have been widely used in heavy metal adsorption studies to evaluate adsorption efficiency at varying pollutant loads (Gupta *et al.,* 2015).

Effect of Competing Ions
The influence of competing ions on adsorption performance was investigated using combined solution of sodium chloride and calcium Chloride. 0.1 M of each interfering salt was prepared and 20 ml of each ion was introduced into the metal solution before adsorption and experiments were conducted under optimized conditions. The residual concentrations of lead, nickel and cobalt were measured using FAAS after filtration, consistent with wastewater interference studies reported (Zang *et al.,* 2019).

Adsorption of Heavy Metals from Industrial Wastewater
Wastewater samples were collected in 1.0 L clean polyethylene containers in triplicate from local cloth-dyeing area in Hadejia, Jigawa State, stored under ice, transported to the Sule Lamido University Chemistry laboratory and preserved at 4^0C in the refrigerator before used for adsorption experiments within 24 hours of collection. The samples were filtered and analysed by AAS to determine the initial concentrations of Pb(II), Ni(II) and Co(II) in the industrial waste water. Fifty (50) ml of the industrial wastewater was then treated with 200 mg ZnO-nanoparticles under optimized adsorption conditions of pH 6 and contact time of 80 minutes. The mixtures were then filtered and analysed using FAAS to determine the residual concentrations of Pb(II) Ni(II) and Co(II) to evaluate removal efficiency as commonly applied in real wastewater treatment (APHA, 2017).

Calculation of Percentage Removal
The percentage removal of heavy metals was calculated using the standard adsorption efficiency equation based on the difference between initial and equilibrium concentrations studies (Mahdavi *et al.,* 2015)

$$\%\text{Removal}=\frac{\text{Co}-\text{Ce}}{Co}\times 100 \qquad 1$$

Where
Co= initial concentration of the metal ion (mg/L or ppm)
Ce = final concentration of the metal ion (mg/L or ppm)

Calculation of Adsorption Capacity
The adsorption capacity at equilibrium (qe) was calculated using the standard mass balance equation for adsorption systems, (Mahdavi *et al.,* 2015), which is usually used in equilibrium and isotherm.

$$\text{qe}=\frac{\text{Co}-\text{Ce}}{m}\times \text{V} \qquad 2$$

Where
q_e = adsorption capacity (mg/g)
Co = initial concentration (mg/L)
Ce = equilibrium concentration (mg/L)
V = volume of solution (L)
m = mass of adsorbent (g)

Determination of Point of Zero Charge (pH_pzc)
The point of zero charge (pH_pzc) of the green-synthesized ZnO nanoparticles was determined using the pH-drift method. A 0.01 M NaCl solution was used as the background electrolyte. A series of 50 mL portions of the NaCl solution were prepared, and the initial pH values were adjusted to approximately 2, 4, 6, and 8 using dilute HCl or NaOH. Then, 200 mg of ZnO nanoparticles was added to each solution. The suspensions were agitated at room temperature 200 rpm for 80 min to allow interaction between the ZnO surface and the electrolyte. After equilibration, the ZnO nanoparticles were separated from the suspensions, and the final pH of each solution was measured.
The change in pH was calculated using:

$$\Delta pH = pH_{final} - pH_{initial} \qquad 3$$

The values of ΔpH were plotted against the corresponding initial pH values. The pH at which ΔpH = 0 was taken as the point of zero charge (pH_pzc) of the ZnO nanoparticles.

Adsorption Isotherm and Kinetic Evaluation
Adsorption Isotherm Studies
Exactly 200 mg of ZnO-NPs was added to 15 separate Erlenmeyer flasks containing 20 mL of the working solution for reacting for 80 min, with 10, 20, 30, 40 and 50 mg/L Co(II), Pb(II) and Ni(II) at ambient (32 ◦C). The adsorption condition of pH 6, adsorbent dosage of 200 mg, contact time of 80 min were maintained. Before adsorption, the pH of the working solution was adjusted to 6.0 with 0.1 mol/L HCl or NaOH. Langmuir and Freundlich isotherm models were applied to simulate adsorbents for Co(II), Pb(II) and Ni(II) adsorption. The Langmuir and Freundlich adsorption equation are presented in equation 6 and 7 below.
Langmuir isotherm model

$$\frac{C_e}{q_e}=\frac{1}{Q_{max}^0}C_e+\frac{1}{Q_{max}^0\,K_L} \qquad 4$$

Q_{max}^0 (mg/g): maximum adsorption capacity. K_L (L/mg): a constant associated with the affinity of ZnO-Nanoparticles and the adsorbed heavy metal ions.
Freundlich isotherm model

$$log q_e = log K_F + \frac{1}{n}C_e \qquad 5$$

K_F (mg/g)/(mg/L)^n: Freundlich constant. n (dimensionless): Freundlich intensity parameter.

Adsorption Kinetic Studies
Exactly 200 mg ZnO-NPs was added to 15 separate Erlenmeyer flasks containing 20 mL of the working solution with 50 mg/L Co(II), Pb(II) and Ni(II) on a shaker and a magnetic stirrer was dropped in the Erlenmeyer flask at ambient temperature (32 ^{0}C) and 180 rpm for adsorption for 10, 20, 30, 40 and 50 min. The solutions pH were adjusted to 6.0. Pseudo-first-order, pseudo-second-order models were exploited to fit the kinetic experimental data of Co(II), Pb(II) and Ni(II) adsorption by the leaf synthesized Zno-NPs. The pseudo-first-order kinetic model and pseudo-second-order kinetic model were used to fit the adsorption kinetics data using the following equations:
Pseudo-1st-order kinetic model

$$\log(qe-qt) = logqe - \frac{K_1}{2.303} * t \qquad 6$$

K_1: the rate constant of the pseudo-1st-order model (min^{-1})
Where qe and qt (g mg^{-1}) are the amount of adsorption at equilibrium and time t (min)
Pseudo-2nd-order kinetic model

$$\frac{t}{qe} = \frac{1}{K_2\,(qe)^2} + \frac{1}{qe{*}t} \qquad 7$$

K_2: the rate constant of the pseudo-2nd-order model (g $mg^{-1}min^{-1}$)

RESULT AND DISCUSSION

Characterization

X-Ray Diffraction (XRD) Analysis of Leaf Synthesized Zinc Oxide Nanoparticles

Seven sharp XRD peaks of the synthesized ZnO NPs were recorded (Figure 1). The values of lattice spacing (d) corresponding to each diffraction angle with their intensity counts are displayed in Table 1 The peaks located at Bragg's diffraction angles (2θ) of 31.79°, 34.43°, 36.27°, 47.64°, 56.71°, 62.85° and 67.99° were assigned to the miller indices (100), (002), (101), (102), (110), (103) and (112) (Figure 1), crystal planes of hexagonal wurtzite ZnO, in accordance with the joint committee of standards of powder diffraction of ZnO file (JCPDS Card No. 00-036-1451) (Prasad *et al.*, *2000)*. The diffraction results confirmed the crystallization of the synthesized ZnO NPs in the hexagonal wurtzite structure which is the most stable and common form at normal conditions of temperature and pressure (Kołodziejczak-Radzimska & Jesionowski 2014). Moreover, the experimental interplanar spacing 2.813 Å, 2.603 Å, and 2.475 Å were similar with the standard values of JCPDS 2.814 Å (100), 2.603 Å (002), and 2.476 Å (101) for hexagonal ZnO nano structure.

The crystal size of the ZnO nanoparticle was calculated using Debye-scherer equation,

$$D = \frac{K\lambda}{\beta cos\theta} \qquad 8$$

Where β is the full width at half maximum in radians of the diffraction peak, λ is the wavelength of the X-ray from Cu-Kα(1.540560Å), θ is the Braggs angle, and K is the form factor, and which has a value of 0.9.

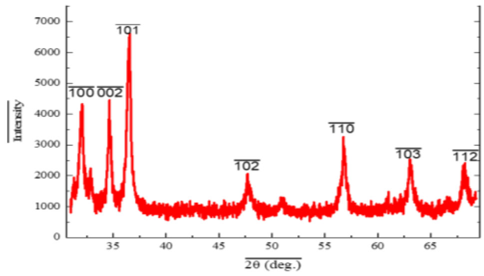

Figure 1: XRD Analysis of Leaf Synthesized Zinc Oxide Nanoparticles

The calculated crystal size of the Zinc oxide nanoparticles ranged from 12.7 to 22.4 nm with an average of size of 16.5 (Table 1).

Table 1: Evaluation of Crystal Size D from XRD Results for the Leaf Synthesized ZnO-Nanoparticles

2θ (°)	θ (°)	FWHM (°)	β (rad)	cosθ	D (nm)
31.79	15.9	0.463	0.00808	0.962	17.9
34.43	17.21	0.371	0.00648	0.955	22.4
36.27	18.13	0.474	0.00827	0.95	17.7
47.64	23.82	0.59	0.0103	0.915	14.7
56.7	28.35	0.583	0.01018	0.88	15.5
62.85	31.43	0.636	0.0111	0.853	14.6
67.99	34.00	0.759	0.01325	0.829	12.7

The XRD analysis of the leaf synthesized nanoparticles confirmed that zinc oxide (ZnO) was the dominant crystalline phase, accounting for approximately 90.3 wt%(JCPDS Card No. 00-036-1451) (Figure 2) of the NPs. The predominance of ZnO indicates that the green synthesis approach effectively converted the zinc precursor into crystalline zinc oxide nanoparticles. However, fluorite and quartz phases were identified in the NPs and accounted for approximately 6.6 wt.% (card number 01-070-1469) and 3.1 wt.% (card number 00-001-0649)(Figure 2), of the crystalline composition respectively. Fluorite is chemically stable in aqueous solution and shows less interaction with dissolved metals. Likewise, quartz was detected in very small amounts and it is relatively inert, it contributes negligibly to adsorption processes compared with ZnO (Fu & Wang, 2011).

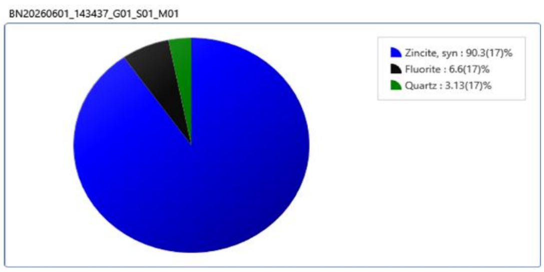

Figure 2: Quantitative Analysis Report of the Leaf Synthesized Zinc Oxide Nanoparticles

The findings of this study are consistent with previous reports on the green synthesis of ZnO nanoparticles. Vijayaraghavan and Ashokkumar (2017) reported highly crystalline hexagonal ZnO nanoparticles synthesized using *Atalantia monophylla* leaf extract, while Elumalai *et al., (*2015) obtained similar diffraction patterns using *Moringa oleifera*. Both studies concluded that plant phytochemicals facilitate controlled crystal growth while minimizing excessive particle agglomeration.

FTIR Analysis Leaf Synthesized NPs

The FTIR spectrum (Figure 3) of the leaf synthesized NPs exhibited characteristics absorption bands at approximately 3384, 1513, 1386, 909 and 551 cm⁻¹. The characteristic Zn–O absorption bands observed at 551 cm⁻¹ provide additional evidence that zinc ions were converted into zinc oxide during the green synthesis (Silverstein *et al.,* 2014).

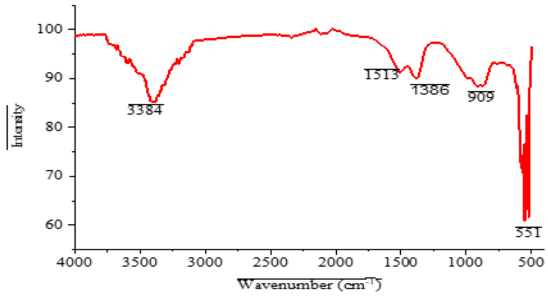

Figure 3: FTIR Analysis of Leaf Synthesized ZnO-NPs

An absorption band was observed at around 3384 cm⁻¹, corresponding to the stretching vibration of hydroxyl (–OH) groups. Hydroxyl groups are commonly associated with phenolic compounds, alcohols present in plant extracts (Silverstein *et al.,* 2014).

Another important absorption peak was observed at approximately 1513 cm⁻¹, corresponding to the stretching vibration of aromatic C=C bonds and, in some cases, amide II vibrations associated with proteins (Ahmed *et al.,* 2016). The absorption band recorded at 1386 cm⁻¹ was assigned to C–N stretching vibrations of aromatic amines or the symmetric stretching of carboxylate groups. Proteins, amino acids, and other nitrogen-containing biomolecules present in plant extracts are known to coordinate with metal ions during nanoparticle formation and subsequently stabilize the resulting nanoparticles (Mittal *et al.,* 2013). While the peak at 909 cm^{-1} was attributed to C = C bending vibration of alkenes or O–H group.

SEM–EDX Analysis of Leaf Synthesized NPs

The surface morphology of the synthesized ZnO NPs was examined by SEM technique. The images (Figure 4) showed that the particles have spherical shapes. In addition, clusters were formed from the aggregation of the spherical granules. A similar particles shape was reported by (Fouladi-Fard *et al.,* 2022) for the preparation of a ZnO nanoparticle by solvothermal process. While Energy-Dispersive X-ray Spectroscopy (EDX) provide a tool used to identify the elemental composition. EDX showed that the predominant elements in the synthesized ZnO NPs are zinc and oxygen. The EDX analysis revealed that zinc and oxygen were the dominant elements present in Leaf synthesized NPs, with zinc accounting for 81.95 wt.% mass percent and oxygen accounted for 17.54 wt.% mass percent (Figure 5).

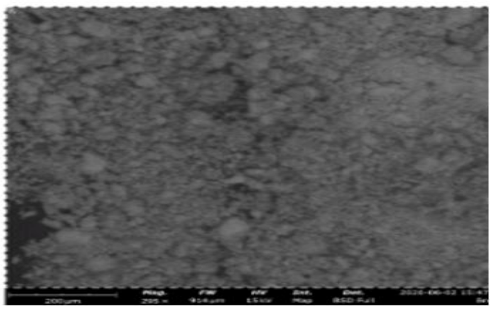

Figure 4: SEM Analysis of Leaf Synthesized ZnO NPs

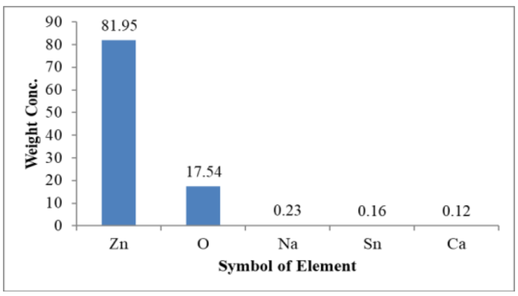

Figure 5: EDX Analysis of leaf Synthesized ZnO NPs

Furthermore, very small amounts of sodium (Na), tin (Sn), and calcium (Ca) were detected. Their respective weight percentages were 0.23%, 0.16%, and 0.12% respectively.

Effect of pH on the Adsorption of Co(II), Pb(II) and Ni(II) ions by Green-Synthesized Leaf-ZnO Nanoparticles

The effect of pH on the adsorption of Co(II), Pb(II) and Ni(II) ions using green-synthesized leaf-mediated ZnO nanoparticles was investigated at pH values of 2, 4 and 6 at ambient temperature by the batch equilibrium approach (Table 2). Also, 200 mg of ZnO-NPs was added to 50 ml containing 20 mg/L of the evaluated metal ion solution. The maximum adsorption of Co(II), Pb(II) and Ni(II) (77.4%, 82.7% and 72.1%, respectively) were achieved at pH = 6. The results are presented in Table 2.

Table 2: The Impact of pH on the % Removal and Metal Adsorption Capacity (mgg^{-1}) of Leaf ZnO NPs

pH		2	4	6
Co(II)	q_e	3.49	3.77	3.87
	% removal	69.8	75.5	77.4
Pb(II)	q_e	2.83	3.57	4.14
	% removal	56.7	71.3	82.7
Ni(II)	q_e	2.82	2.93	3.61
	% removal	56.5	58.5	72.1

Alswata *et al.,* (2017), reported that the small size and the high mobility of hydrogen ions in solutions lead to greater affinity for adsorption on the surface. The high concentration of hydrogen ions at low pH values result to high competition between protons and metal ions for the active sorption sites, and as such low adsorption capacity was observed for the studied metal ions in strong acidic solutions. However, as the at pH increases above 5, the deprotonation of the surface of the adsorbent facilitate the adsorption of the metal ions from the solution. Moreover, the adsorption capacity (qe) values recorded at pH 6 for Co(II), Pb(II) and Ni(II) are 3.87 mgg^{-1}, 4.14 mgg^{-1} and 3.61 mgg^{-1}, respectively for the leaf synthesized NPs were higher than those obtained for pH 2 and 4. This implies high selectivity of ZnO NPs adsorbent for Co(II), Pb(II) and Ni(II) at pH 6. A comparable study by Mostafa *et al.,* (2022) on ZnO nanoparticles reported optimum Pb(II) removal at near-neutral pH due to a similar electrostatic interaction mechanism.

Effect of Contact Time on the Adsorption of Co(II), Pb(II) and Ni(II) ions by Green-Synthesized Leaf-ZnO Nanoparticles

The optimum contact time for the adsorption of Co(II), Pb(II) and Ni(II) by ZnO NPs were assessed at time intervals between 20 and 80 min and under the optimum experimental conditions for each investigated ion. A rapid adsorption of the positive ions on the surface of ZnO NPs was observed at the start of the process which reduced due to the saturation of most of the available active sites as the time increases. The maximum Co(II), Pb(II) and Ni(II) adsorption of 79.0, 69.6 and 84.5%, were recorded at 80 min and metal adsorption capacity of 3.95, 3.48 and 4.22 mgg^{-1}, respectively.

The adsorption trend observed in this study agrees with the findings of Elsharkawy *et al.,* (2024), who reported that adsorption of divalent metal ions onto ZnO-based nanocomposites increased steadily with increasing contact time until equilibrium was established.

Effect of Adsorbent Dosage on the Adsorption of Co(II), Pb(II) and Ni(II) ions by Green-Synthesized Leaf Mediated ZnO Nanoparticles

The effect of adsorbent dosage on the adsorption of Co(II), Pb(II) and Ni(II) ions using green-synthesized leaf mediated ZnO nanoparticles was studied at dosages of 50 mg, 100 mg, 200 mg and 300 mg at the optimum pH value (pH = 6), contact time of 80 minutes and initial metal concentration of 20 mg/L. The results for Co(II) adsorption using the leaf mediated ZnO-NPs showed that the equilibrium concentration decreased from 7.60 mg/L (50 mg) to 7.31 mg/L (100 mg), and then sharply to 1.56 mg/L (200 mg). A slight increase was observed at 300 mg (2.12 mg/L).). In contrast, the adsorption capacity (q_e) decreased steadily from 12.40, 7.35, 4.61 and 2.98 mg/g as the adsorbent dosage increased. Similar behaviour has been reported in ZnO-based adsorption systems where higher dosages improve metal removal due to increased active site availability (Mostafa *et al., 2022*).

When the leaf NPs was evaluated for the adsorption of Ni(II), the equilibrium concentration was observed to decrease from 7.80 mg/L (50 mg) to 6.12 mg/L (100 mg) and further to 2.71 mg/L (200 mg). However, a slight increase was recorded at 300 mg (2.77 mg/L). In contrast, the adsorption capacity (q_e) decreased from 12.20, 6.94, 4.32 and 2.87 mg/g as the adsorbent dosage increased.

Removal efficiency of Pb(II) ions increased with increasing adsorbent dosage from 50 mg (66.7%) to 100 mg (70.0%), and further to a maximum of 200 mg (83.0 %). However, a slight decrease was observed at 300 mg (82.0%), indicating that increasing the adsorbent beyond the optimum level did not significantly improve adsorption performance. The adsorption capacity (q_e) decreased steadily from 13.33, 7.00, 4.15 and 2.73 mg/g as the adsorbent dosage increased.

The results for adsorbent dosage showed that the maximum adsorption capacity for Pb (4.15 mgg^{-1}) was achieved at a sorbent dosage of 200 mg of leaf mediated ZnO NPs. However, the adsorption of Co(II), recorded highest value of 4.61 mgg^{-1} at 200 mg of ZnO NPs. This was followed by NI(II) with a qe value of 4.32 mgg^{-1}. It is important to note that, the small adsorbent dosage required for the maximum removal of Co(II), Pb(II) and Ni(II) ions is a proof of the efficiency of the synthesized ZnO NPs as an adsorbent.

Optimum Concentration

Effect of Initial Metal Concentration on the Adsorption of Co(II), Pb(II) and Ni(II) by ZnO Nanoparticles

The effect of initial Pb(II) concentration on the adsorption performance of leaf-mediated ZnO nanoparticles was investigated using initial concentrations of 10, 20, and 30 mg/L, 40 mg/l and 50 mg/l. The study were conducted under the previously optimized conditions of pH 6, optimum contact time of 80 minutes, adsorbent dosage of 200 mg, and a solution volume of 50 ml, while only the initial Pb(II) concentration was varied.

The results showed that the equilibrium concentration (C_e) increased from 2.46 mg/L at an initial concentration of 10 mg/L to 9.74 mg/L at 20 mg/L, and further to 18.79 mg/L at 30 mg/L, 25.52mg/L at 40mg/L and to 36.10 mg/L at

50mg/L. Consequently, the percentage removal decreased from 75.40% to 51.30%, 37.37%, 36.2% and 27.8% respectively. This indicates that the adsorption efficiency of the leaf synthesized ZnO nanoparticles decreased as the initial Pb^{2+} concentration increased.

Although the percentage removal decreased with increasing initial concentration, the adsorption capacity (q_e) increased from 1.89 mg/g at 10 mg/L to 2.57 mg/g at 20 mg/L, and further to 2.80 mg/g at 30 mg/L, 3.62 mg/g at 40 mg/L and finally to 3.48 mg/g at 50 mg/L. This reveals that a higher initial Pb(II) ions concentration provided a concentration gradient between the metal solution and the adsorbent surface (Remedhan 2020). Furthermore, removal efficiencies of 64.22%, 53.0%, and 47.7%, 40.7% and 28.48% for Ni(II) were recorded at 10 mg/L, 20 mg/L, 30 mg/L, 40 mg/L and 50 mg/L respectively, while the adsorption capacities were 1.60 mg/g, 2.95 mg/g, and 3.58 mg/g, 4.07 mg/g and 3.56 mg/g. Also, 77.8%, 60.5%, 58.60% 50.0% and 43.6% were obtained for Co(II) at 10mg/L, 20mg/L, 30mg/L, 40mg/L and 50mg/L respectively, and the adsorption capacities were 1.94 mg/g, 3.02 mg/g, 4.39 mg/g, 5.00 mg/g and 5.45 mg/g. This trend agrees with the study of (Al-Arjan *et al.,* 2022).

Effect of Interfering Ions on the Adsorption of Co(II), Pb(II) and Ni(II) by Leaf- ZnO Nanoparticles

The influence of interfering ions on Co(II) adsorption by the green-synthesized ZnO nanoparticles was examined using 0.1 M NaCl and 0.1 M $CaCl_2$ under the previously optimized conditions. The adsorption study was carried out at pH 6, a contact time of 80 min, an adsorbent dosage of 200 mg and an initial Co(II) concentration of 20 mg L^{-1}

The equilibrium concentration of Co(II) decreased from 4.210 mg/L in the absence of interfering ions to 3.265 mg/L after addition of the same electrolytes, giving an increase in removal efficiency from 75.54% to 81.03%. The study indicated that the presence of interfering ions increased the adsorption efficiency of the adsorbent.

The presence of interfering ions significantly reduced Pb(II) adsorption under the optimized conditions of pH 6, 80 min contact time, 200 mg adsorbent dosage, and 20 mg/L initial Pb(II) concentration, the equilibrium concentration increased from 6.09 mg/L to 10.756 mg/L, with removal efficiency decreasing from 70.24% to 42.85%. This shows that more Pb(II) ions remain in solution. The equilibrium concentration of Ni(II) increased from 3.103 mg/L to 6.162 mg/L, while the removal efficiency declined from 83.65% to 67.53%.

Adsorption Using Industial Wastewater

Adsorption of Lead from Industrial Wastewater Using the Leaf Synthesized ZnO-Nanoparticles

To evaluate the applicability of the synthesized ZnO nanoparticles, adsorption study were conducted using industrial wastewater collected from Hadejia, Jigawa State, and treated under the optimum adsorption conditions established in this study. The initial Pb^{2+} concentration in the untreated wastewater was 1.20 mg/L and after treatment with the leaf-mediated ZnO nanoparticles it reduced to 0.38 mg/L, corresponding to a removal efficiency of 68.33%. These results indicate that the adsorbent was effective in reducing Pb^{2+} ions concentration in the wastewater matrix. The adsorption capacity for NPs was 0.185mg/g.

Though, the adsorption efficiency decreased in the industrial wastewater matrix, the adsorbent still demonstrated significant adsorption efficiency under environmental conditions. This shows that the green-synthesized ZnO nanoparticles performed favourably in the presence of competing ions and organic pollutants.

Adsorption of Nickel from Industrial Wastewater Using the Leaf synthesized ZnO-Nanoparticles

The adsorption results showed that the adsorbent was effective in removing Ni^{2+} ions from the natural dyeing wastewater, the adsorbent reduced the Ni^{2+} ions initial concentration from 1.156 mg/L to 0.417 mg/L, giving a removal efficiency of 63.92%, This indicates that the adsorbent showed high adsorptive capacity for Ni^{2+} ions in industrial wastewater.

Adsorption of Cobalt from Industrial Wastewater Using the Leaf synthesized ZnO-Nanoparticles

The initial cobalt concentration was 0.960, which decreased to 0.191 after treatment with the adsorbent corresponding to removal efficiencies of 80.10%. Under the optimized conditions of pH 6, adsorbent dose 200 mg and contact time of 80 minutes. As the surface area of the metal oxide NPs increased, the efficiency of the removal of heavy metals also increased.

Adsorption Modeling

Isotherm Models

Langmuir and Freundlich adsorption model were fitted to the adsorption data of Co(II), Pb(II) and Ni(II) ions on ZnO-NPs of the leaf synthesized NPs to correlate the experimental results with the model. The best fitting model displayed a correlation coefficient (R^2) equal to unity Lanjwani *et al.,* (2022). The calculated parameters of the isotherm models were presented in Table 3.

Table 3: Calculated isotherm Model Parameters for the Adsorption of Co(II), Pb(II) and Ni(II) Ions on ZnO- NPs

Equilibrium models	Parameters	Co(II)	Pb(II)	Ni(II)
	q_{max} Expt	3.67	3.84	3.06
Langmuir	q_{max} (mgg^{-1})	6.789	3.862	4.158
Leaf-NPs	K_L (Lmg^{-1})	0.138	0.246	0.279
	R^2	0.9763	0.975	0.9687
Freundlich	K_f(Lmg^{-1})	2.07	2.546	1.448
	n_f (g/L)	2.353	4.16	2.734
Leaf-NPs	$1/n_f$ (Lg^{-1})	0.425	0.2404	0.3657
	R^2	0.9743	0.9364	0.8047
	K_f(Lmg^{-1})	2.356	2.919	1.569

The results revealed that the experimental data for the adsorption of Co(II), Pb(II) and Ni(II) on leaf- synthesized ZnO-NPs fitted well to the Langmuir isotherm (Figures 6, 8, 10 and Table 3), with a correlation coefficient of R^2 = 0.9763, 0.975 and 0.9687 respectively for the synthesized NPs Similarly, the value of maximum adsorption capacity (q_{max})

of the adsorption of Co(II) was the highest which almost double that of Pb(II) ions and it is 1.632 times greater than the value recorded for Ni(II). Moreover, the separation factor R_L indicates that the adsorption is adaptable to the Langmuir isotherm (Torab-Mostaedi *et al.,* 2015).

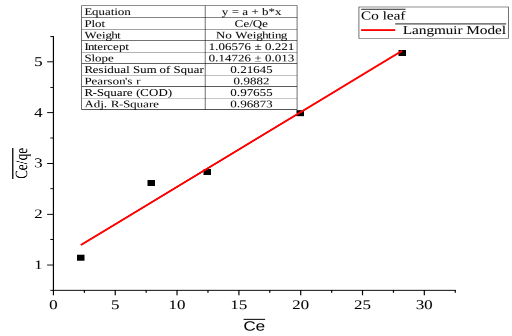

Figure 6: Langmuir Isotherm Model for Co(II) Adsorption by Baobab Leaf Synthesized ZnO NPS

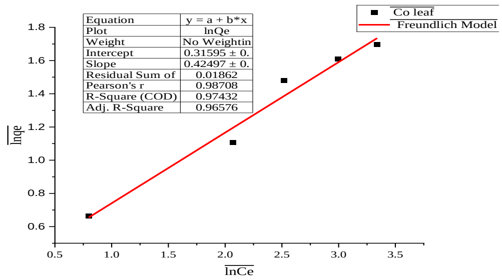

Figure 7: Freundlich Isotherm Model for Co(II) Adsorption by Baobab Leaf Synthesized ZnO NPS

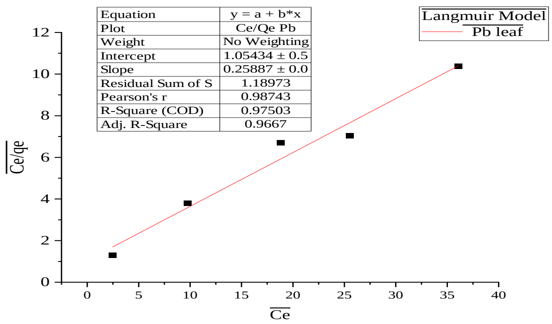

Figure 8: Langmuir Isotherm Model for Pb(II) Adsorption by Baobab Leaf Synthesized ZnO NPS

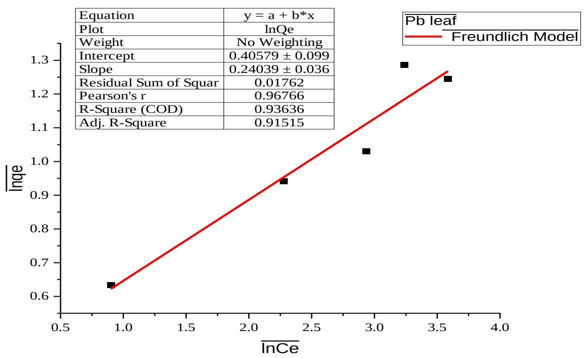

Figure 9: Freundlich Isotherm Model for Pb(II) Adsorption by Baobab Leaf Synthesized ZnO NPS

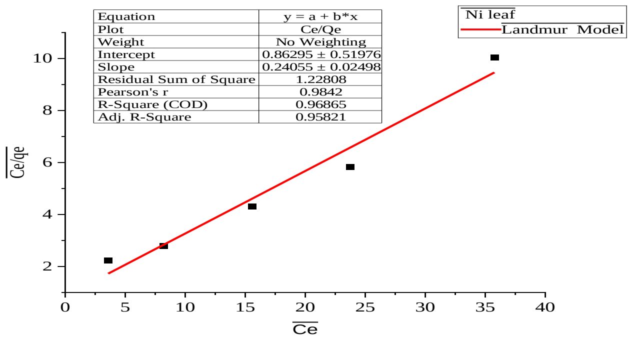

Figure 10: Langmuir Isotherm Model for Ni(II) Adsorption by Baobab Leaf Synthesized ZnO NPS

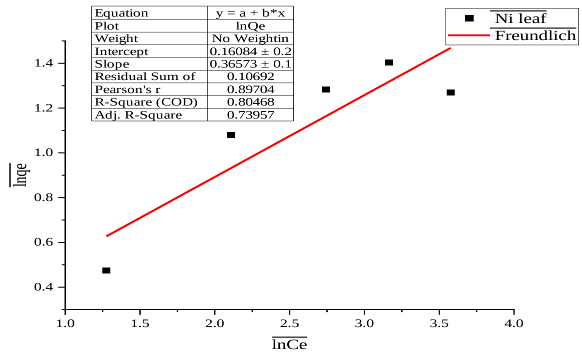

Figure 11: Freundlich Isotherm Model for NiII) Adsorption by Baobab Leaf Synthesized ZnO NPS

Furthermore, the experimental data gave a good fit to Freundlich isotherm (Figures 7, 9, 11 and Table 3), with R^2 = 0.9743, 0.9364 and 0.8047 for Co(II), Pb(II) and Ni(II) ions on ZnO-NPs of the leaf mediated synthesis. The value of the adsorption intensity (*n*) for Co(II), Pb(II) and Ni(II) ions were greater than one, this signify the ease of ions separation from solution which enhances and adsorption (Torab-Mostaedi *et al.*, 2015).

Point of Zero Charge (pHpzc)

The pHpzc of the synthesized ZnO nanoparticles was determined using the experimental results at a pH range of 2 to 8. Moreover, a pHpzc of 6.00 was obtained for the leaf-mediated ZnO nanoparticles. This was deduced from the graph where the change in pH (ΔpH) was zero at pH 6 (Figure 12). The leaf-ZnO NPs reaches its zero-charge point at pH 6. Thus, below this value, the surface of the adsorbent is more protonated, whereas increasing the pH enhances deprotonation of surface of the adsorbent and a shift towards a negatively charged surface.

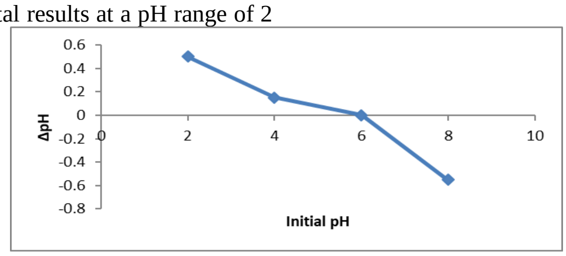

Figure 12: pH Point of Zero Charge (pHpzc) for ZnO-L

Adsorption Kinetics Modelling study

It is vital to use adsorption theories to study the characteristics of ZnO-nanoparticles adsorbent in order to improve its performance and provide a better controlled condition for the treatment of wastewater (Habila *et al.*, 2023).

The pseudo-first-order kinetic model was presented in (Table 4), it can be observed from this table that the calculated adsorption capacity was 0.492, 4.593 and 1.013 mg/g for Co(II), Pb(II) and Ni(II) respectively, which were significantly different from the recorded experimental adsorption capacity values of 3.25, 3.18 and 3.97 mg/g for Co(II), Pb(II) and Ni(II) respectively. The pseudo-second-order model has a relatively high R^2 values when compared with the pseudo-first-order model (Table 4). The highest R^2 value obtained for pseudo-second-order was for Ni(II) (0.998), whereas the calculated qe values for pseudo-second-order kinetic were similar to qe, exp.

Table 4: The Pseudo-First-Order and Pseudo-Second-Order Constants for Adsorption of Co(II), Pb(II) and Ni(II) onto ZnO-Nanoparticles (at an Optimum pH of 6 and Adsorbent Dose of 200 mg)

Metal	qe, exp (mg/g)	qe, Cal. (mg/g)	k_1 (min^{-1})	R^2	qe, Cal. (mg/g)	k_2 (g/mg.min)	R^2
Co(II)	3.25	0.492	0.00740	0.945	3.38	0.05181	0.989
Pb(II)	3.18	4.593	0.04498	0.807	4.96	0.00431	0.832
Ni(II)	3.97	1.013	0.03843	0.819	4.15	0.05845	0.998

However, the pseudo-second-order kinetic model (Table4) showed that the values of 3.38, 4.96 and 4.15 mg/g for Co(II), Pb(II) and Ni(II) respectively, obtained for the calculated adsorption capacity showed no statistical difference from the experimental adsorption capacity values of 3.25, 3.18 and 3.97 mg/g for Co(II), Pb(II) and Ni(II) respectively, as the calculated t value (1.285) was less the critical value (2.920) at $p<0.05$. Moreover, a similar result was reported but (Xingjie *et al.,* 2023). As a result, the pseudo-second-order model was more suitable for describing the adsorption process. These results revealed that the adsorption process onto the developed ZnO-nanoparticles took place in three stages. The first one is by the migration of Co(II), Pb(II) and Ni(II) in the adsorption solution and the second was their arrangement at the ZnO-nanoparticles surfaces whereas the third was their migration through the pores (Mohamed *et al.,* 2014).

Discussion

The FTIR spectra obtained in the present study provided evidence of functional groups associated with the synthesized Zn-O NPs. The FTIR analysis gave a band which corresponds to the Zn–O stretching vibration, this band is widely accepted as the characteristic fingerprint of zinc oxide nanoparticles synthesis. A similar observation was reported by (Zidan *et al., 2022*), who synthesized ZnO nanoparticles using *Ocimum tenuiflorum* leaf extract.

The XRD patterns obtained in this study confirmed the crystalline nature of the synthesized Zn-O NPs. The results are comparable with those of Kane *et al*. (2020), who reported crystalline ZnO nanoparticles synthesized using *A. digitata* leaf extract and demonstrated that extraction conditions could influence the structural characteristics of the obtained ZnO nanoparticles. Similarly, (Zidan *et al.,* 2022) reported the formation of crystalline ZnO with a hexagonal wurtzite structure following green synthesis using *O. tenuiflorum* extract.

The SEM-EDX results provided additional evidence for the formation of the synthesized ZnO nanoparticles through the detection of zinc and oxygen as the principal constituent elements.

The adsorption experiments showed that solution pH had an important influence on the removal of Pb(II) Ni(II) and Co(II) ions. It was observed that, removal efficiency increased as the solution pH increased from 2 to 6, with the highest adsorption obtained at pH 6 within the range investigated. Similar increases were observed for Co(II) and Ni(II), indicating that adsorption was less favourable at strongly acidic conditions. The relatively low removal at pH 2 can be attributed partly to competition between H^+ ions and the dissolved metal ions for available surface sites.

Moreover, the importance of pH in ZnO-NPs heavy-metal adsorption has also been reported by (Akpomie *et al.,* 2023), who identified surface charge, metal-ion speciation and surface interactions as important factors controlling adsorption. (Thao *et al.,* 2022) also reported that pH strongly influenced Pb(II) adsorption by green-synthesized ZnO nanoparticles.

The pHpzc values obtained in this study are important for understanding the adsorption of Pb(II), Ni(II), and Co(II). Surface charge influences how metal ions interact with the available sites on an adsorbent. The increase in metal removal observed with increasing pH can be related to the decreasing concentration of competing H^+ ions and the gradual deprotonation of surface functional groups. Similar pH-dependent adsorption behaviour has been reported for green-synthesized ZnO nanoparticles by (Singh *et al.,* 2024). The present findings are also in agreement with the report of (Canbaz *et al.,* 2024), who investigated green-synthesized ZnO nanoparticles for Cu(II) removal. Their study included pHpzc analysis and showed that surface properties and solution pH were important factors controlling the adsorption process.

The effect of contact time showed that adsorption increased as the interaction between the ZnO nanoparticles and metal ions was increased. The initial increase in metal uptake can be associated with the availability of numerous adsorption sites at the beginning of the experiment. As adsorption proceeds, an increasing proportion of these sites become used up and the rate of adsorption gradually decreases as the process get to equilibrium.

The effect of adsorbent dosage showed that increasing the amount of ZnO nanoparticles generally improved the percentage removal of the metal ions up to an optimum level. At the same time, adsorption capacity per unit mass decreased as the adsorbent dosage increased (Zidan *et al.,* 2022). The increase in removal efficiency can be explained by the greater number of available adsorption sites associated with the increased mass of adsorbent. However, when the amount of adsorbent becomes excessive relative to the amount of metal available in solution, some adsorption sites may remain used.

Initial metal concentration also affects the adsorption process. The percentage removal decreased as the initial concentration increased, whereas the amount of metal adsorbed per unit mass increased. These observations are not inconsistent. At lower concentrations, the number of metal ions present in solution is relatively small compared with the number of available adsorption sites, allowing a larger proportion of the dissolved metal to be removed. At higher concentrations, the adsorption sites become progressively occupied, resulting in a lower percentage removal. This type of concentration-dependent behaviour is consistent with the adsorption principles discussed by (Banerjee *et al.,* 2011) and with the concentration-dependent behaviour reported for green-synthesized ZnO in the study of (Kalaiselvie *et al.,* 2015).

The adsorption equilibrium results showed that the Langmuir model provided the better fit for the adsorption process. The relatively high Langmuir R^2 values suggest that the equilibrium data for these systems were well described by the Langmuir model, which assumes adsorption onto a finite number of energetically similar sites and formation of an adsorbed layer.

The predominance of the Langmuir model is consistent with the review of (Ain *et al.,* 2013), which examined adsorption mechanisms and modelling of heavy metals and radionuclides on ZnO nanoparticles.

The influence of competing ions further demonstrated that adsorption performance was affected by the composition of the aqueous medium. The presence of dissolved salts reduced the removal of the target metal ions, indicating ionic-strength effects as well as the effect of competing ions. Pb(II) for instance, interfering ions increased the equilibrium concentration and reduced the removal efficiency under the optimized conditions. Such behaviour is expected in complex aqueous systems because competing cations may occupy available surface sites, while increased ionic strength can alter electrostatic interactions between dissolved metal ions and the adsorbent surface.

The results obtained using industrial wastewater provides an important indication of the practical potential of the synthesized ZnO nanoparticles. Unlike the single-metal synthetic solutions, industrial wastewater contains a mixture of dissolved ions and other constituents that may compete for adsorption sites. The ability of the adsorbents to remove the investigated metals ions under these more complex conditions demonstrates that the NPs were efficient in the removal of these metals from aqueous solution.

This findings demonstrate that the green-synthesized ZnO nanoparticles were effective for the removal of Pb(II), Ni(II) and Co(II) from aqueous solutions. The adsorption performance was strongly influenced by pH, contact time, adsorbent dosage, initial metal concentration and the presence of competing ions.

CONCLUSION

The XRD results confirmed the crystallization of the synthesized ZnO NPs in the hexagonal wurtzite structure. Also, the FTIR analysis gave a band which corresponds to the Zn–O stretching vibration, this band is widely accepted as the characteristic fingerprint of zinc oxide nanoparticles synthesis.

The surface morphology of the synthesized ZnO NPs was examined by SEM technique. The images showed that the particles have spherical shapes. EDX showed that the predominant elements in the synthesized ZnO NPs were zinc and oxygen.

The batch experiments conducted for the three investigated metal ions gave the best performing conditions within the tested range, pH of 6, metal initial concentration of 20 mg/L for Co(II), Pb(II) and Ni(II), contact time (80 min.) and adsorbent dosage (200 mg) of the synthesized ZnO NPs were the best conditions. The effect of interfering salts varied among the metals, enhancing Co(II), removal but reducing Pb(II) and Ni(II) adsorption which may be due to ionic-strength effects as well as the effect of competing ions. The results for the treatment of industrial wastewater for the adsorption of Co(II), Pb(II) and Ni(II) ions achieved removal efficiency of 80.10%, 68.33%, and 63.92%, respectively). Further studies are required to evaluate adsorbent stability, regeneration capacity, and performance using additional wastewater.

DECLARATION OF COMPETING INTEREST

The authors hereby declare that there is no conflicting interest.

REFERENCES

Abirami, S., Kadirvelu, K., & Baskar, S. (2024). Trace Metal Based Eco-Biological and Health Risk Status of Surface Water and Sediments of Noyyal River Basin, Tamil Nadu, India. *Soil and Sediment Contamination: An International Journal,* 33(7), 799–828. https://doi.org/10.1080/15320383.2023.2258234

Ahmed, S., Ahmad, M., Swami, B. L., & Ikram, S. (2016). Green synthesis of silver nanoparticles using *Azadirachta indica* aqueous leaf extract. *Journal of Radiation Research and Applied Sciences*, 9(1), 1–7.

Ain, Q. U., Shah, S. A., & Haq, A. U. (2013). Nanomaterials: A review of synthesis methods, properties, recent progress, and challenges. *Materials Today: Proceedings*, 1(1), 79–90.

Akpomie, K. G., Conradie, J., Adegoke, K. A., Oyedotun, K. O., Ighalo, J. O., Amaku, J. F., Olisah, C., Adeola, A. O., & Iwuozor, K. O. (2023). Adsorption mechanism and modeling of radionuclides and heavy metals onto ZnO nanoparticles: A review. *Applied Water Science,* 13, 20

Al-Arjan, W. S. (2022). Zinc oxide nanoparticles and their application in adsorption of toxic dye from aqueous solution. *Polymers*, 14(15), 3086, 1 - 25.

Alswata, A. A., Ahmad, M. B., Al-Hada, N. M., Kamari, H. M., Hussein, M. Z. B. & Ibrahim, N. A. (2017). Preparation of zeolite/zinc oxide nanocomposites for toxic metals removal from water. *Results in Physics*, 7, 723–731

American Public Health Association, American (APHA) (2017). Water Works Association, & Water Environment Federation. Standard methods for the examination of water and wastewater (23rd ed.). *American Public Health Association*.

Bagheri, M., Azizian, S., Jaleh, B. & Chehregani, A. (2014). Adsorption of Cu(II) from aqueous solution by micro-structured ZnO thin films. *Journal of Industrial and Engineering Chemistry,* 20, 2439–2446.

Banerjee, J. & Narendhirakannan, R.T. (2011). Biosynthesis of silver nano-particles from *Syzygium cumini* (L.) seed extract and evaluation of their in vitro antioxidant activities. *Digest Journal of Nanomaterials and Biostructures,* 6, 961-968.

Boukhemkhem, A., Aissa-Ouaissi-Sekkouti, B., Bedia, J., Belver, C., Molina, C.B., 2022. Adsorption of crystal violet on kaolinite clay: kinetic and equilibrium study using non-linear models. *Clay Miner.* 57 (1), 41–50. http://dx.doi.org/10.1180/clm.2022.18.

Elsharkawy, W. B., Mwafy, E. A., Alghamdi, S. M., Alsubhe, E., Albeydani, O., Mostafa, A. M., Toghan, A., & Rezk, R. A. (2024). Isotherm and kinetics study of Ni(II) ions adsorption from wastewater using carbon nanotubes decorated with ZnO nanoparticles. *Fullerenes, Nanotubes and Carbon Nanostructures,* 32(11), 1005–1016.

Elumalai, K., & Velmurugan, S. (2015). Green synthesis, characterization and antimicrobial activities of zinc oxide nanoparticles from the leaf extract of *Azadirachta indica (L.). Applied Surface Science,* 345, 329–336.

Fouladi-Fard, R., Aali, R., Mohammadi-Aghdam, S., & Mortazavi-Derazkola, S. (2022). The surface modification of spherical ZnO with Ag nanoparticles: A novel agent, biogenic synthesis, catalytic and antibacterial activities. *Arabian Journal of Chemistry*, 15(3), 1-15

Fu, F. & Wang, Q. (2011). Removal of heavy metal ions from wastewaters: A review. *Journal of Environmental Management*, 92(3), 407–418.

Gupta, V. K., Nayak, A., & Agarwal, S. (2015). Bioadsorbents for remediation of heavy metals: Current status and their future prospects. *Environmental Engineering Research*, 20(1), 1–18.

Habila, M. A., ALOthman, Z. A., Hakami, H. M. & Alanazi, A. G. (2023). Influence of Synthesis-Heating Conditions on the Porosity and Per formance of a Carbon Nanotube/SDS-Alumina Nanocomposite for Effective Wastewater Treatment: Fabrication, Characterization, and Adsorption Modeling. *Industrial Engeneering Chemistry. Research*. 62, 12571–12588.

Huang, X., & Chen, Y. (2007). Coagulation behaviors of aluminum sulfate and polyaluminum chloride in synthetic colored wastewater. *Desalination*, 202(1–3), 351–360.

Jha, A. K., Prasad, K., & Kulkarni, A. R. (2009). Synthesis of silver nanoparticles using Cycas leaf and its electrocoagulation application for dye removal. Colloids and Surfaces B: *Biointerfaces*, 73(2), 219–223.

Kalaiselvi, A., Roopan, S.M., Madhumitha, G., Ramalingam, C. and El-ango, G. (2015). Synthesis and characterization of palladium nanopar-ticles using *Catharanthus roseus* leaf extract and its application in the photo-catalytic degradation. Spectrochimica acta. Part A, *Molecular and Biomolecular Spectroscopy*, 135: 116-119.

Kane, A. O., Thior, S., Ndiaye, N. M., Ngom, B. D., & Sakho, O. (2020). Influence of Adansonia digitata leaves dye extraction solvent nature on the structural and physical properties of biosynthesized ZnO nanoparticles. *American Journal of Nanomaterials*, 8(1), 10–17.

Kołodziejczak-Radzimska, A., & Jesionowski, T. (2014). Zinc Oxide—From Synthesis to Application: A Review. *Materials,* 7(4), 2833–2881.

Kumar, R., Umar, A., Kumar, G., & Nalwa, H. S. (2015). Antimicrobial properties of ZnO nanomaterials: A review. *Ceramics International,* 43(5), 3940–3961.

Kumar, S. G., & Rao, K. S. R. K. (2017). Comparison of modification strategies towards enhanced charge carrier separation and photocatalytic degradation activity of metal oxide semiconductors (TiO_2, WO_3 and ZnO). *Applied Surface Science*, 391, 124–148.

Lagergren, S. (1898). Zur Theorie der sogenannten Adsorption gelöster Stoffe. *Kungliga Svenska Vetenskapsakademiens Handlingar,* 24(4), 1–39.

Lanjwani, M. F., Khuhawar, M. Y., Khuhawar, T. M. J., Lanjwani, A. H., Memon, S. Q., Soomro, W. A. & Rind, C, I. K. (2022). Photocatalytic deg radation of eriochrome black T dye by ZnO nanoparticles using multivariate factorial, kinetics and isotherm models. *Journal of Cluster Science* 18:1–2.

Mahdavi, S., Afkhami, A., & Merrikhpour, H. (2015) Modified ZnO nanoparticles with new modifiers for the removal of heavy metals in water. *Clean Technology Environmental Policy* 17(6):1645–1661.

Majeed, S., Danish, M., Ismail, M. H. B., Ansari, M. T. & Ibrahim, M. N. M. (2019). Anticancer and apoptotic activity of biologically synthesized zinc oxide nanoparticles against human colon cancer HCT 116 cell line- in vitro study. *Sustain Chem Pharm* 14:100179.

Masoud, M. S., Zidan, A. A., E. l., Zokm, G. M., Elsamra, R. M. I., Okbah, M. A. (2022). Humic acid and nano-zeolite NaX as low cost and eco-friendly adsorbents for removal of Pb (II) and Cd (II) from water: characterization, kinetics, isotherms and thermodynamic studies. *Biomass Conver Biorefin*. Doi: https://doi.org/10.1007/s13399-022-02608-9

Mittal, A. K., Chisti, Y., & Banerjee, U. C. (2013). Synthesis of metallic nanoparticles using plant extracts. *Biotechnology Advances*, 31(2), 346–356.

Mohamed E. A., Habila, M.A., Abbas, I. M., Puzon, L. J., ALOthman, Z. A. (2014). Simple and Facile Synthesis of Amino Functionalized Hollow Core–Mesoporous Shell Silica Spheres Using Anionic Surfactant for Pb (II), Cd (II), and Zn (II) Adsorption and Recovery. *Chemical Engineering Journal*, 251, 441–451.

Monda, H., Ndikubwimana, T., & Hatakeyama, M. (2011). Biosynthesis of metal oxide nanoparticles using plant extracts: A green chemistry approach. *Journal of Environmental Nanotechnology,* 1(2), 43–53.

Moreira V. R., Lebron Y.A.R., Lange L.C., Santos L.V.S. (2019). Simultaneous biosorption of Cd (II), Ni (II) and Pb (II) onto a brown macroalgae *Fucus vesiculosus*: Mono-and multi-component isotherms, kinetics and thermodynamics. *Journal of Environmental Management*, 251: 109587, 10.1016/j.jenvman.2019.109587

Mostafa, N. G., Yunnus, A. F., Elawwad, A., & Kyzas, G. (2022). Adsorption of Pb(II) from water onto ZnO, TiO_2, and Al_2O_3: Process study, adsorption behaviour, and thermodynamics. *Adsorption Science & Technology,* 7582756.

Muhammad R., M., Yahya, R., Hassan, M. S., & Othman, N. H. (2021). A review on green synthesis of zinc oxide nanoparticles using plant extracts and microbial synthesis. *Journal of Photochemistry and Photobiology,* 43–53

Prasad, M., Amritphale, S., Saxena, S., & Chandra, N. (2000). Attenuation of heavy metal ions by lean grade phosphorite. *Minerals Engineering*, 13(12), 1301–1305.

Rajkumari, J., & Sanatombi, K. (2017). Green synthesis of zinc oxide nanoparticles using Camellia sinensis leaf extract and their antibacterial activity. *Materials Today: Proceedings,* 4(9), 3179–3185.

Remedhan, S. T. (2020). Experimental investigation of thermodynamics, kinetics, and equilibrium of nickel ion removal from wastewater using zinc oxide nanoparticles as the adsorbent. *Engineering and Technology Journal*, 38(7A), 1047–1061.

Shah F., S., Jan, H., Shah, S. A., Shah, S., Khan, A., Akbar, M. T., Rizwan, M., Jan, F., Wajidullah, Akhtar, N., Khattak, A., & Syed, S. (2021). Green synthesis of zinc oxide (ZnO) nanoparticles using aqueous fruit extracts of Myristica fragrans: Their characterizations and biological and environmental applications. *ACS Omega*, 6(14), 9709–9722.

Sharma, B. & Shukla, P. (2021). Lead bioaccumulation mediated by *Bacillus cereus* BPS-9 from an industrial waste contaminated site encoding heavy metal resistant genes and their transporters. *Journal of Hazardous Materials*, *401:* 401, 123285, 10.1016/j.jhazmat.2020.123285

Siddiqi, K. S., ur Rahman, A., Tajuddin, & Husen, A. (2018). Properties of zinc oxide nanoparticles and their activity against microbes. *Nanoscale Research Letters*, 13, 141.

Silverstein, R. M., Webster, F. X., Kiemle, D. J., & Bryce, D. L. (2014). Spectrometric Identification of Organic Compounds (8th ed.). Wiley.

Singh, A. K., Hussain, A., Priyadarshi, M., & Haider, A. (2024). Heavy metals removal from synthetic and industrial wastewater using synthesized zinc oxide nanoparticles. *Journal of the Indian Chemical Society,* 101(5): 101 – 145

Thao, T. T., Tam, K. T., Thom, N. T. H., & Tuan, N. T. (2022). Green synthesis of ZnO Nanoparticles using Piper chaudocanum L. Leaf Extract : Characterization and its Application in Pb(II) adsorption. *VNU Journal of Science: Natural Sciences and Technology*, 38(3): 45 – 53

Torab-Mostaedi, M., Ghassabzadeh, H., Ghannadi-Maragheh, M., Ahmadi, S. J., & Taheri, H. (2010). Removal of cadmium and nickel from aqueous solution using expanded perlite. *Brazilian Journal of Chemical Engineering*, 27(2), 299–308.

Vijayaraghavan, K., & Ashokkumar, T. (2017). Plant-mediated biosynthesis of zinc oxide nanoparticles using Atalantia monophylla leaf extract and evaluation of their biological activities. *Journal of Photochemistry and Photobiology B: Biology*, 177, 250–258.

Xingjie, L., Zhigang, Z., Qiusheng, X., Ning, H., Jiejie, K., Daofeng, Z., Rungen, L., Qin, S. (2023). Potential application of Curtobacterium sp. GX_31 for efficient biosorption of Cadmium: Isotherm and kinetic evaluation. *Environmental Technology and Innovation*, 30, 103 – 112

Zang, L., Lin, R., Dou, T., Wang, L., Ma, J., & Sun, L. (2019). Electrospun superhydrophilic membranes for effective removal of Pb(II) from water. *Nanoscale Advances*, 1(1), 389–394.

Zidan, A. A., El Zokm, G. M., & Okbah, M. A. (2022). Green synthesis of nanostructured zinc oxide by Ocimum tenuiflorum extract: Characterization, adsorption modeling, cytotoxic screening, and metal ions adsorption applications. *Biomass Conversion and Biorefinery*, 14, 16843–16856

.